Carbon-Negative Nickel Mining to Meet Global Mineral Resource Demands

Quin R.S. Miller [a*], Alexandra B. Nagurney [a1], Madalyn S. Blondes [b2*], Joyashish Thakurta [c], Jian Liu [a], Greeshma Gadikota [d], Nabajit Lahiri [a], H. Todd Schaef [a]

[a] Energy and Environment Directorate, Pacific Northwest National Laboratory, Richland, Washington, USA
[b] Geology, Energy, & Minerals Science Center, U.S. Geological Survey, Reston, Virginia, USA
[c] Natural Resources Research Institute, University of Minnesota Duluth, Duluth, Minnesota, USA
[d] School of Civil and Environmental Engineering, Cornell University, Ithaca, New York, USA

[1] Current affiliation is ION Clean Energy
[2] Current affiliation is Carbfix

KEYWORDS: in situ mining, resource exploration, critical minerals, critical mineral recovery, carbon mineralization, nickel

ABSTRACT: CO_2-Enhanced Mineral Recovery (CO_2-EMR) is a deep in situ mining technology that utilizes an engineered CO_2 leaching fluid to extract nickel (Ni) and cobalt (Co) from subsurface ultramafic rocks, while simultaneously permanently mineralizing CO_2 as carbonate minerals. This carbon negative process can contribute to meeting the mineral demands of current and emerging energy technologies. We calculate the amount of Ni and Co available for recovery, and carbon mineralized via this technology from a generic ultramafic intrusion and 14 ultramafic intrusions globally. If 5% of a 1 km^3 olivine rock volume reacts with injected CO_2, that will yield 500,000 MT Ni, 21,000 MT Co, and store 100 MMT of CO_2. Further, 130,000 MMT of Ni, or 2,600x the Ni required for the cumulative global production of energy storage batteries through 2050, are stored in ultramafic rocks in the United States. Globally, the Tamarack Bowl, United States and Savannah Intrusion, Australia have the greatest internal return rate for economic profitability.

1. INTRODUCTION

Emerging energy and computing technologies requires the mining and production of over 20 critical materials and minerals(IEA, 2021). Critical minerals (i.e. Ni, Cu, Co, Li, Pt, REEs) are a subset of critical materials that are defined by the United States Energy Act of 2020 as a mineral or element that has a high risk of supply chain destruction and serves an essential function in energy technologies(Energy, 2023). Nickel (Ni) is a key critical mineral, as it is an important component of batteries(Trost and Dunn, 2023) used in electric vehicles, Artificial Intelligence (AI) data centers, smart grid storage, and advanced robotics. Driven by policy and consumer uptake, electric vehicle sales are predicted to increase as much as 25x 2020 sales by 2050(IEA, 2021), which equates to 50 million tons of Ni required to produce the necessary batteries(Hund et al., 2020). Ni is conventionally sourced from high-grade laterite and magmatic sulfide deposits, which globally contain at least 350 million metric tons (MMT) of Ni(Mudd and Jowitt, 2022). In 2022, 3.3 MMT of Ni were produced from laterite (70%) and sulfide (30%) ores, with 50% of production concentrated in Indonesia, Philippines, and Russia(IEA, 2021; McRea, 2023). It presents a risk to have a few countries control the global supply of a critical minerals, as supply and price will be closely linked to physical disruptions, geopolitical events, and regulations there(IEA, 2021).

Additionally, there are environmental issues associated with current Ni mining practices that highlight the challenges faced in an increasingly carbon- and water- constrained world. This challenge has catalyzed recent interest in coupling critical material mining with carbon management approaches. (Gao et al., 2023; Gazzetti et al., 2023; Hamilton et al., 2020a; Hamilton et al., 2018a; Hamilton et al., 2020b; Hamilton et al., 2018b; Honda-McNeil, 2022a, b; Jacobs et al., 2025; Katre et al., 2024; Li et al., 2023; Murchland et al., 2023; Polites et al., 2022b; Power et al., 2024b; Santos et al., 2015; Stanfield et al., 2024; Wang et al., 2024; Wang and Dreisinger, 2022a, c, 2023a, b; Wang et al., 2023a; Wang et al., 2023b; Wicks and King, 2021; Wilson and Hamilton, 2022; Wilson et al., 2023; Zhang et al., 2025) The mining industry is responsible for 4-7% of global greenhouse gas (GHG) emissions(Delevingne, 2020). Other effects of Ni mining include: forest clearing, which can reduce biodiversity(Dickinson and Berner, 2010), smelting of sulfur rich ores that increases particulates that contribute to acid rain(Mudd, 2010), acid mine drainage from tailings, which may pollute the local water and have negative effects on human, plant, and animal life(Simate and Ndlovu, 2014), and dam tailings failures that can bury homes and release trace metals into the ecosystem(Quaresma et al., 2021). An increasingly water-constrained world experiencing significant volatility in freshwater availability from year to year, with some areas of the world undergoing shortages, emphasizes the importance of reducing water usage in emerging extractive industries(Brown et al., 2019). These environmental issues directly impact the communities surrounding the mines, as exemplified in Indonesia(Morse, 2019).

To mitigate these challenges while producing the necessary Ni new technology, new mining technologies need to be developed that account for: i) increasing demand for Ni, driven by electric vehicle production, ii) diversifying where the Ni is mined to mitigate geopolitical and environmental effects, iii) decreasing the emissions associated with mining, iv) minimizing the negative environmental consequences of mining, and v) increasing cost effectiveness. We introduce a CO_2-Enhanced Mineral Recovery (CO_2-EMR) process that permanently mineralizes

CO_2 in subsurface ultramafic rocks while bringing Ni rich fluids to the surface (**Figure 1**). CO_2-EMR is an in situ, carbon negative, nickel mining technology that utilizes an engineered CO_2 based fluid that can be deployed in most magmatic ultramafic rocks, which are distributed globally. These rocks contain abundant (>50%) olivine [(Mg, Fe)$_2$SiO$_4$] with 500 – 5,000 ppm Ni(Barnes et al., 2023). For magmatic ultramafic rocks, the Ni-content of olivine is primarily determined by the initial amount of Ni in the magma and timing of sulfide saturation in the magma, and, moreover, there is a positive correlation, in general, between the Ni-content and Mg-content in olivine(Barnes et al., 2023; Morfin et al., 2024).

In the proposed technology, CO_2 is injected into subsurface ultramafic rocks at depths > 800 m, at conditions which CO_2 may be in either the liquid or supercritical state, depending on the formation temperature and local geothermal gradient. Upon the reaction of CO_2 with olivine, most cations (Mg, Fe, Mn) will form stable carbonate minerals with the CO_2, while Ni will be released into the fluid phase (**Figure 1**)(Bobicki et al., 2015; Kelemen and Matter, 2008; Li et al., 2018; Matter and Kelemen, 2009; Wang and Dreisinger, 2022b; White et al., 2020). The formation of carbonate minerals, without forming detectable Ni-carbonates has been demonstrated in laboratory

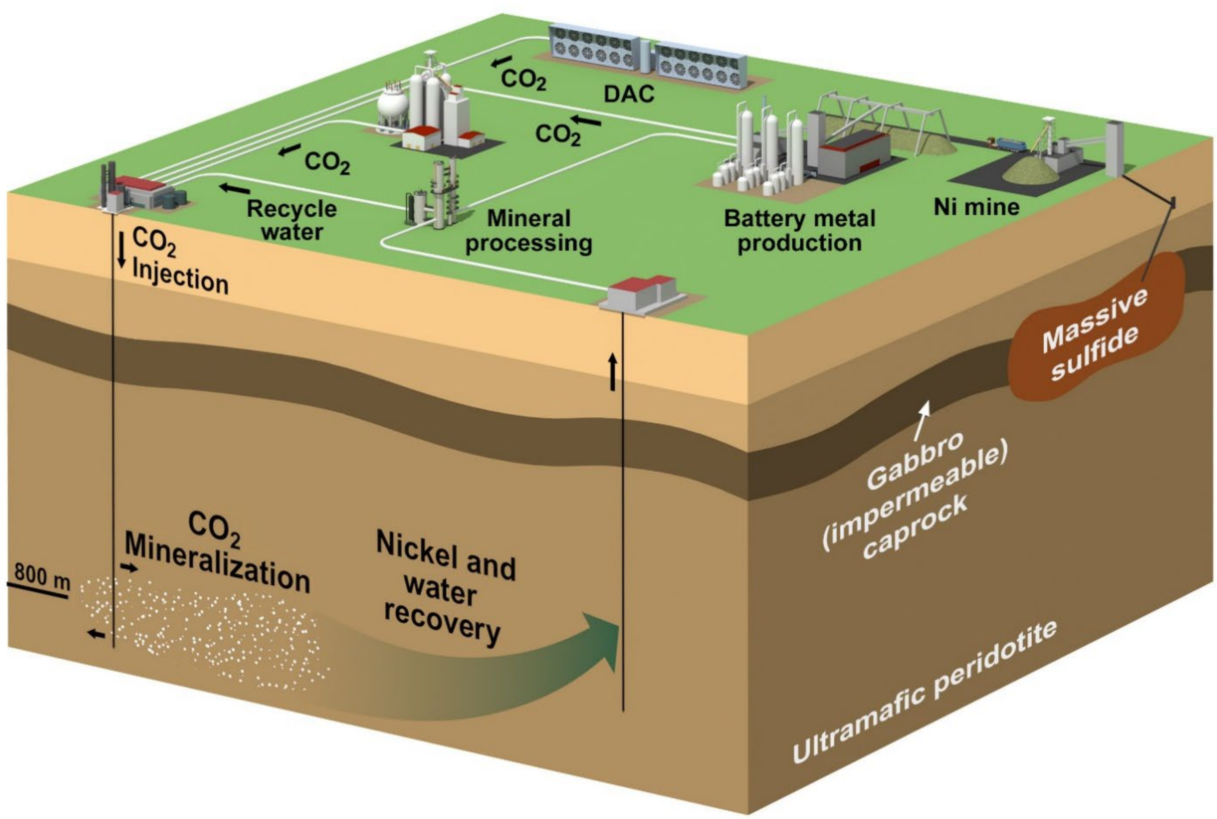

Figure 1. Overview of proposed CO_2-Enhanced Mineral Recovery (EMR) technology implemented at a nickel sulfide mine. CO_2 is injected into, and Ni recovered from ultramafic rocks. This exists in parallel to mining of high-grade nickel in massive sulfide ore. Above ground mining infrastructure includes high grade Ni mine, recovered Ni and water processing, and battery metal production. CO_2 emissions from processing and production are captured and stored prior to injection underground. A Direct Air Capture (DAC) facility on site increases capacity for CO_2 injection.

experiments on olivine carbonation in water rich environments(Wang and Dreisinger, 2022b). Ni can then conceivably be extracted and processed for use in electric vehicles, high performance AI data centers, and other industries that need high performance Ni batteries. CO_2-EMR builds upon successful demonstrations of CO_2 injection into subsurface basalts and laboratory testing of ex situ mineralization of ultramafic mine tailings(Depp et al., 2022; Hamilton et al., 2020b; Lahiri et al., 2023; Matter et al., 2016; McGrail et al., 2017; Pogge von Strandmann et al., 2019; Polites et al., 2022a; Power et al., 2024a; Snaebjornsdottir et al., 2020; White et al., 2020; Wilson et al., 2014). The proposed technology will ideally target ultramafic rock formations that contain an impermeable caprock (**Figure 1**), thereby reducing concerns about the impact of mining operations on groundwater, as the caprock allows reactions to occur isolated from the groundwater table.

CO_2-EMR will permanently mineralize CO_2 in underground reservoirs while simultaneously extracting critical minerals from the target asset. A key component of this technology is that it will be deployed in low grade ultramafic rocks instead of high-grade Ni sulfide ores. This offers multiple advantages relative to traditional, high-grade Ni mining. In situ subsurface leaching will reduce hazardous mine tailings piles and associated acid mine drainage. The global distribution of magmatic ultramafic rocks also allows for the widespread distribution of this technology, potentially reducing geopolitical effects associated with a few countries controlling the commodity supply and increasing production to allow Ni supply to keep pace with future demand(IEA, 2021). Finally, high-grade Ni sulfide ores that are currently mined are hosted in ultramafic rocks, so it will be possible to utilize already existing infrastructure for high-grade Ni sulfide mining for the CO_2-EMR technology in the surrounding ultramafic rocks (**Figure 1**).

Herein, we first calculate the amount of Ni that can be extracted and CO_2 mineralized in a generic 1 km^3 ultramafic rock volume and then apply that methodology to 14 global ultramafic intrusions. Then, we estimate the amount of Ni potentially recoverable from low-grade ultramafic rocks in the United States. Taken together, these results highlight the enormous potential for critical mineral recovery and carbon mineralization in ultramafic rocks to meet the mineral demands for new technologies and unleashing new energy technologies.

2. METHODS

Initial Intrusion Characteristics: The initial intrusion is a 1×10^9 m^3 (V_{rock}) block of ultramafic rock (dunite) and the proportion of olivine in the rock (X_{Ol}) is 1.0(Miller et al., 2002). Initial Ni content of olivine (X_{Ni}) is 3000 ppm, which is an average estimate for a Fo_{90} olivine composition(Barnes et al., 2023).

Total Amount of Ni Produced and CO_2 Stored: The total amount of Ni that could be produced ($m_{Ni,tot}$, g), and CO_2 stored ($m_{CO_2,tot}$, g) in that 1 km^3 block of olivine was calculated based on the mass (m_{rock}, g) and moles (mol_{rock}) of the rock, the molas mass of CO_2 (M_{CO_2}, 44.01 g), and 2 moles of carbonate formed for every mole of forsterite consumed (Equation 1) via Equations 2 and 3. This calculation assumes that the entire block of olivine will react with CO_2 to form carbonate minerals and amorphous silica via Equation 1.

$$Mg_2SiO_4 + 2CO_2 = 2MgCO_3 + SiO_{2_{am}} \quad (1)$$

$$m_{Ni,tot} = m_{rock} * X_{Ni} \tag{2}$$

$$m_{CO_{2,tot}} = mol_{rock} * 2 * M_{CO_2} \tag{3}$$

120 **2.3 Fraction Reactive Rock.** Considering that it is unlikely that 100% of any intrusion will react
121 with injected CO_2, we determined the fraction of reactive rock (X_{RR}) that will react with the
122 injected CO_2 is 0.05 (**S1)**. From there, using density (ρ, g/cm^3), molar mass of forsterite (M_{Fo}), the
123 mass of reactive rock (m_{RR}), moles of reactive rock (mol_{RR}) (Equations 4 & 5), and amount of Ni
124 produced (m_{Ni}) and CO_2 stored (m_{CO_2}) (Equations 6 & 7) were calculated as follows:

$$m_{RR} = V_{rock} * X_{RR} * \rho \tag{4}$$

$$mol_{RR} = \frac{m_{RR}}{M_{Fo}} \tag{5}$$

$$m_{Ni} = m_{RR} * X_{Ni} \tag{6}$$

$$m_{CO_2} = mol_{RR} * 2 * M_{CO_2} \tag{7}$$

125 **Integrating Rates into the Equation.** While the calculations presented above are useful for
126 understanding the total amount of Ni produced from and CO_2 stored in an ultramafic intrusion, the
127 addition of rate equations to the calculations can determine the total amount of time it would take
128 for each of the following processes to occur: injection of CO_2 into the intrusion, dissolution of
129 olivine, and crystallization of carbonate minerals. The addition of rate equations, and therefore
130 time, also allows us to understand the economic and commercial viability of the proposed
131 technology. A discussion of these rates and the rate limiting step is in **S2.**

132 The CO_2 injection rate is a value that takes into account multiple variables including: number of
133 injection wells, CO_2 injection rate per well, and various technological processes including well
134 design, etc. The CO_2 injection rate equivalent to the amount of CO_2 emitted by a 1,000 MW gas-
135 fired powered plant is 43 kg / s(Jayne et al., 2019). For these calculations, the CO_2 injection rate
136 (r_{inj}, kg/s) was increased to 60 kg / s, which is still a reasonable injection rate. This has an
137 equivalent rate of 1.90 MMT / year.

138 To determine the timescales of reaction, we calculated the time to inject the amount of CO_2 (t, yr)
139 that could transform into carbonate minerals, assuming 5% of the rock reacts (Equation 8). From
140 there, the amount of CO_2 stored based on injection rate ($m_{CO_2,inj}$, g) (Equation 9) was calculated.
141 The amount of Ni produced was then determined as in Equation 6. In this calculation, it is assumed
142 that the reaction goes to completion, the CO_2 comes into contact with, and reacts with 5% of the
143 rock volume, and the Ni released from the olivine is completely dissolved into the aqueous fluid
144 and does not precipitate or form any metal ion complexes (Wang and Dreisinger, 2022b), and there
145 is no loss of CO_2 from the rock volume. There are 3.15 x 10^7 seconds / year.

$$t = \frac{m_{RR} * 2 * M_{CO_2} * 3.15x10^7}{r_{inj}} \tag{8}$$

$$m_{CO_{2,inj}} = t * r_{inj} * 3.15x10^7 \tag{9}$$

Global Evaluation of Ultramafic Intrusions Calculations. To evaluate the potential of the proposed technology on real world locations, we calculate the amount of Ni that can be produced and CO_2 that can be mineralized in 14 mafic-ultramafic intrusions, some of which that are associated with Ni-Cu-Co-PGE mineralization, worldwide. Many of these intrusions are either currently being mined for high grade ore, or there are plans to develop mining in that area. The initial focus is on smaller volume intrusions that are well suited for the construction of the proposed technology (**Figure 1**). Smaller volumes allow for less of an above ground footprint of a single well and nearby mineral processing facility.

Descriptions of these intrusions are in **S3**. The calculations were done in the same manner as the generic case, with a few key differences. First, it is challenging to accurately determine the total volume of ultramafic intrusions in the subsurface as that relies on drill core and cross section interpretations of the intrusions. Therefore, instead of determining the total volume of each intrusion, we compare the CO_2 storage and Ni production potential from one injection site into a 1 km^3 block of 14 ultramafic intrusions of variable mineralogy and olivine composition.

Values for proportion of olivine in the rock and Ni content of olivine were determined from the literature (**Table 1**). The starting fraction of reactive rock (X_{RR}) was updated to consider the proportion of olivine in the rock (X_{Ol}), where $X_{RR} = 0.05 * X_{Ol}$. Then, the total amount of Ni produced was calculated as Equation 6 and amount of CO_2 stored as in Equation 9. For each intrusion, a low and high value for CO_2 mineralized and Ni produced was calculated. The low values were determined by utilizing the low end of the range for olivine in the rock and the amount of Ni in olivine. The high values were determined in the same manner. This produces a range of values for CO_2 stored and Ni produced.

Internal Rate of Return (IRR). To understand the economic benefits and risks of this technology, an internal rate of return calculation was conducted. The capital costs including well drilling, water pumping, and CO_2 compressing were estimated assuming a 900 m main well with 3 horizontal branch wells. The operating costs were estimated by adding the material costs, utility (electricity and water), and labor costs. Based on this cost information, a discounted cash flow method was used to determine if an investment was worthwhile in which the IRR was calculated when the net present value of all cash flows was equal to zero(Hartman and Schafrick, 2004; Peters et al., 2002). The assumed operating time is 30 years which is the length of time for CO_2 storage as well. Assuming the investors expect the double the invested cash in 5 years, the internal return rate (IRR) needs to be 15%. A 15% IRR was selected as a target to assess the ability to make a profit with reasonable rate for Ni mining in each case as previously mentioned. If the annual CO_2 storage amount is 1 MMT, the minimum Ni productivity was calculated to be 2,913 MT / year to meet the 15% IRR target. No cost or credit was assumed for CO_2 used and sequestered in this analysis. The 2022 commodity price for Ni metal ($25/kg Ni) was used for Ni metal products in the calculation. Other financial parameters were from an ARPA-e economic analysis tool(Liu et al., 2021) and the cost model from the literature(Liu et al., 2021) and the interest rate was updated to 6.0%.

In this analysis, a higher IRR indicates that it will take less time to recover the capital investment and to make a net profit. A negative IRR value indicates that the case will lose money. For some cases, the IRR is not applicable (N/A) because the productivity of Ni is so low that cash flow is negligible.

Life Cycle Assessment. To evaluate the extent to which the CO_2-EMR technology represents a carbon negative mining process, we conducted a Life Cycle Assessment (LCA) based on the function unit of making 1 kg of Ni using the proposed supercritical CO_2 extraction method. The inputs are CO_2, water, chemicals and energy and the outputs are Ni, brine waste and solid waste. The Eagle Intrusion was chosen for the LCA example, as the Eagle Mine is the only operating nickel mine in the United States.(Clarke et al., 2023)

Table 1. Name, location, rock type, volume % olivine and Ni in olivine data for 14 ultramafic intrusions.

Name	Location	Rock Type	Minimum Values		Maximum Values	
			Volume % Olivine	Ni in Olivine (ppm)	Volume % Olivine	Ni in Olivine (ppm)
Jinchuan (Chai and Naldrett, 1992)	China	Peridotite	40	1515	80	2485
Ban Phuc (Glotov et al., 2001)	Vietnam	Serpentinized Dunite	45	200	65	3600
Eagle (Ding et al., 2010)	United States	Olivine Melatroctolite	30	1750	45	2250
Tamarack (Taranovic et al., 2015)	United States	Bowl Intrusion	60	2480	70	3050
Tamarack (Taranovic et al., 2015)	United States	CGO Intrusion	20	1760	50	3890
Noril'sk 1 (Li et al., 2003)	Russia	Picritic Gabbro	20	1222	50	2230
Talnak (Li et al., 2003)	Russia	Picritic Gabbro	20	1754	50	1949
Nkomati (Li et al., 2002)	South Africa	Main Harzburgite	10	2456	50	4691
Savannah (Le Vaillant et al., 2020)	Australia	Peridotite	40	2000	90	3100
Eagle's Nest (Mungall et al., 2010)	Canada	Lherzolite	10	1000	70	3000
Kevitsa (Luolavirta et al., 2018)	Finland	Olivine Pyroxenite	10	100	35	3650
Luanga (Mansur and Ferreira Filho, 2016)	Brazil	Harzburgite	10	4770	50	6083
Duke Island (Thakurta et al., 2008)	United States	Dunite	80	888	95	2444
Kabanga (Maier et al., 2010)	Tanzania	Harzburgite	10	900	50	1800

The weathering reaction of olivine in the presence of CO_2 is irreversible, and has been generally described Eq. 10(Donaldson, 1985)

$$Mg_2SiO_4 + 4CO_2 + 4H_2O \rightarrow 2Mg^{2+} + 4HCO_3^- + H_4SiO_4 \qquad (10)$$

The CO_2 emission from the energy consumption to extract Ni, the CO_2 embedded in the chemicals, and the CO_2 emission from the handling of wastes were estimated using the normalized consumption or generation rate and the unit CO_2 emission for each source. The solid waste emission was estimated from the landfilled municipal solid waste and the brine waste emission was estimated from the brine management emission penalty(Bartholomew and Mauter, 2021; Verma and Borongan, 2022). The electricity was assumed to be generated using natural gas and the CO_2 emission is about 0.93 kg/kWh. The embedded CO_2 in sulfuric acid was estimated based on the electrolytic production method (0.2 kWh/mol)(Lammers et al., 2023). It is assumed that based on experimental work(Wang and Dreisinger, 2022b), a chelating agent (1,3-propylenedinitrilotetraacetic acid, PDTA) will be injected to aid in the Ni recovery process. The embedded CO_2 in PDTA was assumed to be 2 times of the acetic acid which is 1.0 kg CO_2/kg acetic acid(2012).

2.8 United States Nickel Abundance Estimate. To determine the amount of nickel in ultramafic rocks in the United States ($m_{Ni,US,tot}$, g), the volume of ultramafic rocks in the United States (V_{US}, km^3), the average nickel content of those rocks ($X_{Ni,US}$), and the ultramafic mineral proportion of those rocks were determined (X_{UM}). First, the total volume of ultramafic rocks in the United States were estimated (**S4**).

Second, the average bulk rock nickel content of ultramafic rocks was determined by querying the EarthChem PetDB database for bulk rock compositions from ultramafic rocks worldwide. The data were downloaded from the PetDB Database (http://www.earthchem.org/petdb) on 7 & 10, July 2023, using the following parameters: sample type: igneous: plutonic: ultramafic, and wehrlite, websterite, pyroxenite, peridotite, olivinite, lherzolite, harzburgite, dunite, and clinopyroxenite and sample type: metamorphic, and metaperidotite and serpentinite. The average bulk rock nickel content is 1850 ppm Ni. Bulk rock nickel content was chosen for this analysis instead of nickel in olivine to account for varying degrees of serpentinization of ultramafic rocks. Serpentinization processes will reduce the proportion of olivine in the rock as it reacts to serpentinite minerals, however, the nickel formerly in olivine will be redistributed into other mineral phases, remaining as part of the bulk rock composition.

Third, the total amount of nickel in ultramafic rocks in the United States was calculated in Equation 10, if at least 70% (by volume) of the ultramafic rocks consist of Mg-silicate minerals like olivine and serpentinite group minerals.

$$m_{Ni,US,tot} = V_{US} * X_{Ni,US} * X_{UM} \qquad (10)$$

3. RESULTS AND DISCUSSION

CO_2-EMR Potential in a Generic Rock. To explore the full potential of the proposed CO_2-EMR technology, we calculate two parameters for a generic 1 km^3 volume of a generic ultramafic rock that is 100% olivine and contains 3000 ppm Ni in olivine: i) the amount of Ni that can be recovered and ii) the amount of CO_2 that can be mineralized. If 100% of that rock reacts, that 1 km^3 dunite could produce 10 MMT Ni and store 2,000 MMT CO_2. However, if only 5% of the 1 km^3 block of olivine reacts with CO_2, the total amount of Ni produced, and CO_2 stored in the block of olivine is 500,000 MT Ni and 100 MMT CO_2. If the time to inject the CO_2 into the subsurface is considered, then, if 5% of the rock reacts, that rock can produce 500,000 MT Ni and store 100 MMT CO_2 over 53 years.

Global Evaluation of Ultramafic Intrusions for CO_2-EMR Technology. The results for the amount of CO_2 stored, Ni produced, and 30 year operating IRR for the 14 ultramafic intrusions are shown in **Table 2**. The minimum values were determined using the low-end of olivine in the rock and Ni in olivine, and the maximum values were calculated based on the high-end values.

Figure 2 shows the maximum potential for CO_2 mineralized, and Ni produced for each of these intrusions. Duke Island Complex, United States and Savannah intrusion, Australia can mineralize

Table 2. Results for CO_2 stored, Ni produced, and 30 year operating internal return rate (IRR) for 14 ultramafic intrusions globally.

Name	Minimum Values				Maximum Values			
	CO_2 Stored (MMT)	Time to Inject CO_2 (yr)	Ni Produced (MT)	30-Yr IRR	CO_2 Stored (MMT)	Time to Inject CO_2 (yr)	Ni Produced (MT)	30-Yr IRR
Jinchuan	40	21	100,000	18%	80	42	330,000	51%
Ban Phuc	45	24	15,000	N/A	65	34	390,000	70%
Eagle	30	16	88,000	15%	45	24	170,000	38%
Tamarack	60	32	250,000	51%	70	37	360,000	62%
Tamarack	20	11	59,000	2%	50	26	330,000	69%
Noril'sk 1	20	11	41,000	-15%	50	26	190,000	42%
Talnak	20	11	59,000	2%	50	26	160,000	35%
Nkomati	10	5	41,000	-10%	50	26	390,000	78%
Savannah	40	21	130,000	28%	90	48	470,000	62%
Eagle's Nest	10	5	17,000	N/A	70	37	350,000	60%
Kevitsa	10	5	1,700	N/A	35	19	210,000	49%
Luanga	10	5	80,000	16%	50	26	510,000	95%
Duke Island	80	42	120,000	10%	95	50	390,000	51%
Kabanga	10	5	15,000	N/A	50	26	150,000	33%

the greatest amount of CO_2 with the proposed technology. Luanga, Brazil and Savannah, Australia, will produce the greatest amount of Ni.

The differences in the amount of CO_2 mineralized in the intrusions is based on the amount of olivine in the rock. Intrusions with greater amounts of olivine are thereby capable of mineralizing more CO_2. The differences in Ni produced between the intrusions is based on both i) the amount of olivine in the rock and ii) the amount of Ni in olivine. For example, a large volume of rocks in Savannah and Duke Island have very high amounts of olivine (90-95%) (**Table 1**), thereby allowing for the greatest amount of CO_2 mineralized. Savannah has a greater amount of Ni in olivine than Duke Island (3,100 vs. 2,444 ppm). Therefore, Savannah will produce more Ni. Luanga only has 50% olivine, but the olivine is highly enriched in Ni (6083 ppm). Therefore, Luanga will produce the most Ni, but not mineralize the most CO_2. For comparison, Kabanga has the same volume % olivine as Luanga, (50%), but only 1,800 ppm Ni in olivine. These intrusions will both mineralize 50 MMT CO_2, but Luanga will produce significantly more Ni, due to the concentration of Ni in olivine. These comparisons show that olivine abundance and composition are key to determining the utility of the CO_2-EMR technology in any given intrusion.

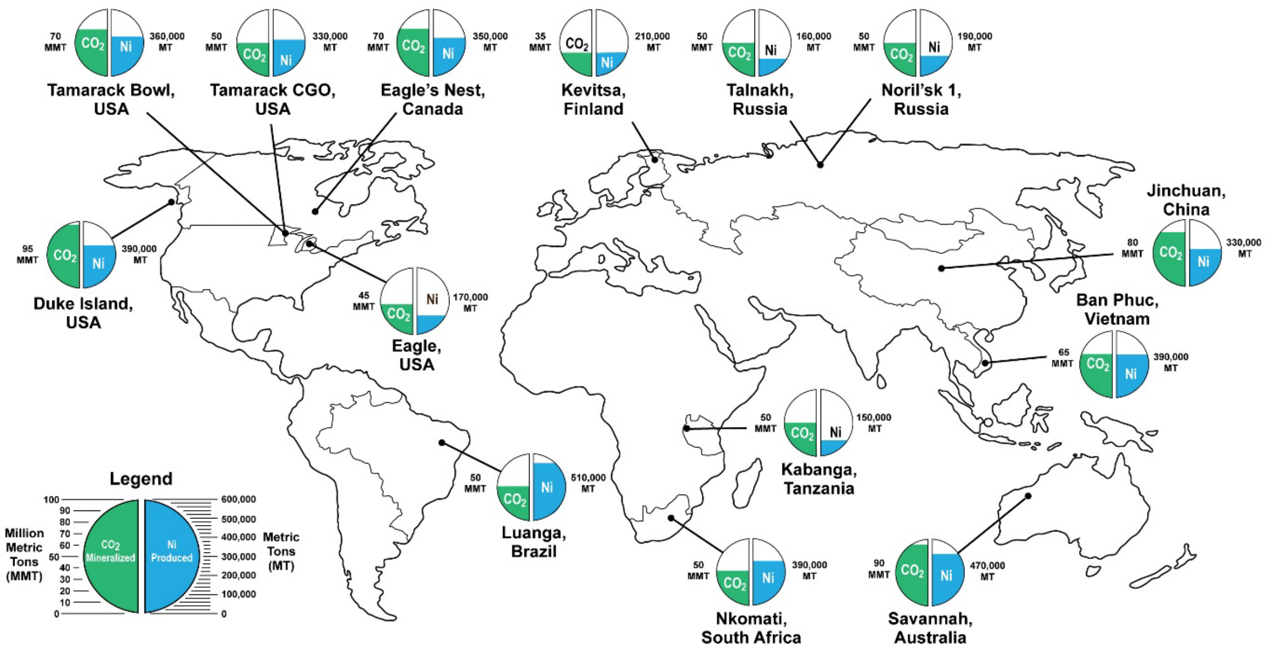

Figure 2. Maximum values for CO_2 mineralized and Ni produced from the CO_2-EMR technology from 14 ultramafic intrusions worldwide.

All 14 intrusions meet the internal return rate (IRR) target of >15% when the concentration of Ni in olivine is at or near its measured maximum value (**Table 2**). However, most cases cannot meet the IRR target when the concentration of Ni in olivine is at or near its minimum value. Of the 14 global target assets, Jinchuan, Eagle, Tamarack Bowl, Savannah and Luanga have a >15% 30-year Ni IRR for both the minimum and maximum cases. However, the Tamarack Bowl and Savannah have the greatest 30-year Ni IRR for both the minimum and maximum cases, and therefore are the most economically attractive targets to deploy the CO_2-EMR technology are these two localities.

Life Cycle Assessment for Carbon-Negative Mining. The Eagle Intrusion was used as a case study to determine the extent of the carbon negative mining process, considering CO_2 emissions from the mining process. **Table 3** shows the results for the net CO_2 emissions of the CO_2-EMR process for both the minimum and maximum amounts of CO_2 storage and Ni produced. For the Eagle Intrusion, the amount of CO_2 stored when extracting 1 kg of Ni ranges from 334.8-647 kg depending on the amount of olivine in the rock and the Ni in olivine content. Based on the LCA calculation, **Table 3** shows that for both the minimum and maximum values of CO_2 stored and Ni produced, the net CO_2 emissions are negative. It is interesting to note that the net CO_2 emissions are actually greater for the minimum scenario than the maximum scenario. This is the result of olivine abundance (which controls the amount of CO_2 mineralized) not scaling directly with the Ni in olivine content (which controls the amount of Ni produced). The net CO_2 emission for the maximum CO_2 storage and Ni production case is lower due to higher Ni concentration and productivity. However, the key takeaway remains- this is a net carbon negative mining process.

Additionally, when considering all other ultramafic intrusions (**Table 1-2**), in all cases, in both the minimum and maximum scenarios, the net CO_2 emission to produce 1 kg is always negative. Therefore, for all the sites, the CO_2-EMR technology is a carbon-negative way to mine Ni.

United States Nickel Abundance Estimate. The results for individual intrusions in **Table 2** and **Figure 2** are useful for thinking about this technology in terms of individual intrusions and mine sites. However, to understand the full potential of this technology ultramafic rocks to source Ni, we calculate the total amount of Ni hosted in ultramafic rocks in the United States. This is motivated by the fact that the Unites States has only one operating Ni mine, the Eagle Mine, MI, which is set to close in the next ~10 years after the high grade ore is exhausted(Clarke et al., 2023).

Therefore, the United States needs additional domestic supply of Ni, which may be able to come from ultramafic rocks which cover ~1% of the surface of the United States(Krevor et al., 2009). We calculate, based on the volume of ultramafic rocks, their bulk rock Ni content, and the proportion of Mg-silicate minerals in the rock, the total amount of Ni hosted in igneous and metamorphic ultramafic rocks in the United States. These ultramafic rocks contain up to 130,000 MMT of Ni, over 370 times more than the 350 MMT of identified Ni resources hosted in high-grade sulfide and laterite deposits worldwide(Mudd and Jowitt, 2022).

For comparison, 50 MMT of Ni are cumulatively required to meet the demand for energy storage batteries by 2050 based on the International Energy Agency's Below 2°C Scenario (IEAB2DS2)(Hund et al., 2020). Therefore, ultramafic rocks in the United States contain 2,600x more Ni than is needed for the global production of batteries through 2050. Ultramafic rocks, which are traditionally considered a waste rock in the mining process, can be a source for Ni both domestically in the United States and globally, and may be capable of producing the Ni necessary for current and emerging technologies if they can be mined via surgical in situ mining processes.

Potential Deployment Locations and Pathways to Commercialization. The results above inform the geologic and technologic factors that will aid in selection of ultramafic intrusions for deploying the CO_2-EMR technology. Selecting for intrusions that contain abundant (> 60%) olivine and Ni rich (> 3,000 ppm) olivine will allow for the maximization of both the CO_2 mineralized and Ni produced from an intrusion. Other variables, such as CO_2 injection rate and % reactive rock can be technologically altered. Increasing the injection rate of CO_2 into the subsurface is possible through either faster pumping or adding multiple injection wells into the same rock volume. Increasing the amount of reactive rock is possible through fracturing technologies, which would increase both the amount of CO_2 that could be mineralized, and Ni produced from an ultramafic intrusion.

High-grade Ni-sulfide mines offer an ideal location for the deployment of the CO_2-EMR technology as the ultramafic host rocks are normally well characterized, and the drilling infrastructure and processing facilities can be updated for the CO_2-EMR technology while reducing capital cost (**Figure 1**). Further, the development of Direct Air Capture (DAC) technologies allows for the separation of CO_2 injection sites from point source CO_2 emitters. Deploying DAC technology near the CO_2 injection sites reduces the need for pipelines(Küng et al., 2023). However, the cost of CO_2 capture for the DAC technologies are higher and the combined effect to the cost of CO_2-EMR need to be evaluated. Facilities for the extraction and processing of the critical mineral rich fluid must be developed for the CO_2-EMR technology to reach commercial scale. To reduce the land surface footprint and costs of the mining process, these facilities could ideally be integrated into current mine operating infrastructure (**Figure 1**). In addition, it is possible to extract Cobalt (Co) in addition to Ni via hydrometallurgical processes, which may provide additional revenue(Friedrich et al., 2020).

Comparison to High Grade Ni-Sulfide Mining and CO_2 Mineralization in Ultramafic Mine Tailings. The high-grade Ni-sulfide ore produced at the Eagle Mine, MI, United States, can be compared to the potential Ni produced and CO_2 stored via the CO_2-EMR technology in the surrounding rock. In 2022, the Eagle Mine produced 18,000 MT Ni(McRea, 2023). The CO_2-EMR technology, deployed in a 1 km^3 volume of olivine melatroctolite surrounding the high-grade Ni-sulfide at Eagle, will produce 88,000-170,000 MT of Ni over 16-24 years, equating to 2,900 – 5,700 MT Ni / yr (**Table 1**), assuming 100% recovery of the Ni from the fluid. On a per year basis, this is less Ni than the high-grade Ni sulfide mine will produce. However, this technology,

Table 3. Life Cycle Assessment

Item	**Minimum CO_2 Storage and Ni Production**	**Maximum CO_2 Storage and Ni Production**
Ni productivity (kg/hr)	334.8	647.0
CO_2 storage rate (kg CO_2/kg Ni)	341.6	264.9
Total CO_2 storage rate (MT/yr)	1,001,786	1,501,058
H_2O usage rate (m^3/kg Ni)	0.065	0.050
Sulfuric acid (kg/kg Ni)	0.36	0.28
PDTA* (kg /kg Ni)	0.036	0.028
Grid electricity (kWh/kg Ni)	3.1	2.1
Brine waste (kg/kg Ni)	0.18	0.07
Solid waste (kg/kg Ni)	0.32	0.25
CO_2 emission from process energy (kg/kg Ni)	1.3	0.9
CO_2 emission from Solid waste (kg/kg Ni)	0.25	0.20
CO_2 emission from Brine waste (kg/kg Ni)	0.012	0.004
CO_2 emission from Chemicals (kg/kg Ni)	0.85	0.66
Net CO_2 emission of the process (kg/kg Ni)	***-339.2***	***-263.1***

deployed at a Ni-sulfide mine, may allow the mine to continue producing Ni after the high-grade ore is exhausted, highlighting how the CO_2-EMR process can be deployed as a complement to high-grade mining operations.

The best current state of the art comparison to the CO_2-EMR technology for CO_2 mineralization is the Mount Keith Nickel Mine, Australia, where 39,800 tons / year of atmospheric CO_2 are passively carbonated in ultramafic mine tailings(Hamilton et al., 2020b; Hamilton et al., 2018b). Assuming a constant rate of passive carbonation, over a 30-year period, 1.1 MMT of CO_2 will be mineralized in ultramafic tailings at the Mount Keith Nickel Mine. In comparison, the CO_2-EMR technology will store >50 MMT of CO_2 in situ over a 30-year period at ultramafic intrusions (**Table 2**), offering a benefit over the current state of the art technology.

Co-Production of Other Critical Minerals. Another benefit to the proposed CO_2-EMR technology is that it has the potential to co-produce other critical minerals. Co is present in olivine at ~125 ppm(Herzberg et al., 2016), is a key component of battery technologies(IEA, 2021), and there is demand for new sources of Co, as traditional Co mining, concentrated in the Democratic Republic of Congo, has undergone scrutiny for environmental and social reasons(Gulley, 2022). Therefore, it may be possible for the CO_2-EMR technology to co-produce Co in addition to Ni. Based on the generic case calculation, reacting 5% of a 1 km^3 block of olivine will produce 21,000 MT of Co. For comparison, in 2022, United States and global production of Co was 800 MT and 190,000 MT, respectively(2023b). Therefore CO_2-EMR, deployed globally, could be an important source of Co in addition to Ni.

Potential Impediments and Solutions to Full Scale CO_2-EMR Operation. Commercial scale CO_2-EMR operations requires accurate characterization of ultramafic intrusions, optimization of injection strategies, and mitigation of environmental and human health risks. Accurate characterization of the target rock body is key to determining the economic feasibility of deploying CO_2-EMR. Therefore, well characterized intrusions should be targets of this technology.

The composition of the injection fluid and behavior of the fluid in the subsurface must be optimized via laboratory testing prior to field scale injection. Further, the reactivity of the rock with CO_2 can be decreased via the precipitation of passivating layers on reactive surfaces, or alternatively increased via reaction induced fracturing(Bearat et al., 2006; Kelemen and Hirth, 2012)[cite Lafay 2018]. Clogging versus cracking processes should be tested in the laboratory prior to field scale injection and further parameterized via reactive transport reservoir modeling. At the field scale, monitoring technologies can aid in determining the rates and migration of the injected CO_2-rich and critical mineral-rich fluids(White et al., 2020). In recent years, driven by earthquakes in Oklahoma, induced seismicity from subsurface fracturing is an issue that has undergone increasing attention in the public sphere(Langenbruch and Zoback, 2016). Induced seismicity may also be a challenge for CO_2 sequestration in ultramafic rocks, as rock fracturing technologies will likely be necessary to produce porosity and permeability in these reservoirs. The impacts of induced seismicity may be reduced by altering fluid injection strategies(Zang et al., 2018), along with hazard evaluation and risk informed seismic analysis(Templeton et al., 2021).

Groundwater contamination is a common concern across mining projects. To mitigate groundwater contamination, the United States Environmental Protection Agency (EPA) requirements for a Class VI CO_2 injection well include: computational modeling of the injected CO_2 plume, monitoring and testing of groundwater throughout the lifetime of the project, requirements for plugging the injection well, and a site-specific emergency plan(2023a). Reactive transport models can aid in developing injection strategies that mitigate potential groundwater impacts. Injection of CO_2 into the subsurface into formations below an impermeable caprock will mitigate the potential migration of buoyant CO_2 into drinking water reservoirs (**Figure 1**)(Snaebjornsdottir et al., 2020). Other challenges include avoiding the dissolution of sulfides(Schaef et al., 2013), which may be of particular concern in ultramafic rocks that have high concentration of sulfide minerals and the production of methane and H_2S gases from microbial interactions with CO_2(Guyot et al., 2011). Here, characterization of the rocks to avoid sulfur rich target reservoirs, lab scale experiments, and reactive transport models can be used to determine the fate of dissolved sulfides and production of disadvantageous gasses prior to field scale injection.

Finally, key to the successful deployment is working within local communities and articulating the benefits of the CO_2-EMR technology. Emphasis should be placed on utilizing existing infrastructure for high grade Ni-sulfide mining to reduce the land footprint of additional mining. This will reduce the costs and community impacts associated with new mining development. Additionally in situ mining mitigates the environmental hazards of mine tailings. These benefits, over ex situ leaching or traditional mining must be clearly articulated to community members.

4. Conclusions

To secure a sustainable and secure supply chain for emerging energy and computing technologies, development of novel critical mineral exploration, extraction, and processing technologies is necessary. The proposed CO_2-EMR technology could play a key role in this mission, as it allows for the extraction of Ni, Co, and potentially other critical minerals from ultramafic rocks, while permanently storing CO_2 in the subsurface. This deep in situ mining practice will have a significantly reduced environmental footprint compared to traditional mining practices while also unlocking new targets for exploration and production. This process can be implemented globally, therefore diversifying suppliers of critical minerals, and accelerating the production of technologies required for a low carbon future. Emissions from mine processing plants and associated transportation can be captured through point air capture technologies, making the mine site itself carbon negative. This can be further coupled with DAC to further reduce atmospheric carbon dioxide, and the cost of CO_2 capture through 45Q Tax Credits. This coupled process of utilizing CO_2-based leaching fluids while producing critical minerals distinguishes CO_2-EMR as a key technology for unlocking new types of ore grades and mining targets.

AUTHOR INFORMATION

*Corresponding Authors

Quin R.S. Miller, quin.miller@pnnl.gov
Madalyn S. Blondes, mblondes@usgs.gov

ACKNOWLEDGMENTS

This study was supported by Dr. Douglas Wicks (DOE HQ) and the DOE Advanced Research Projects-Energy (ARPA-e) MINER program under contract No. 22/CJ000/09/02.This work was performed at the Pacific Northwest National Laboratory (PNNL), with DOE HQ support from Dr. Douglas Wicks and the Department of Energy (DOE) Advanced Research Projects-Energy (ARPA-e) MINER program under contract No. 22/CJ000/09/02. We thank Michael Perkins (PNNL) for his assistance with preparing the graphics. PNNL is operated by Battelle for the Department of Energy under contract no. DE-AC05-76RLO1830.

REFERENCES

2012. US Life Cycle Inventory Database. National Renewable Energy Laboratory.
2023a. Class VI- Wells used for Geologic Sequestration of Carbon Dioxide, United States Environmental Protection Agency.
2023b. Cobalt, Mineral Commodity Summary.
Barnes, S.J., Yao, Z.-S., Mao, Y.-J., Jesus, A.P., Yang, S., Taranovic, V., Maier, W.D., 2023. Nickel in olivine as an exploration indicator for magmatic Ni-Cu sulfide deposits: A data review and re-evaluation. Am. Mineral. 108, 1-17.
Bartholomew, T.V., Mauter, M.S., 2021. Energy and CO(2) Emissions Penalty Ranges for Geologic Carbon Storage Brine Management. Environ Sci Technol 55, 4305-4313.
Bearat, H., McKelvy, M., Chizmeshya, A., Gormley, D., Nunez, R., Carpenter, R., Squires, K., Wolf, G., 2006. Carbon Sequestration via Aqueous Olivine Mineral Carbonation: Role of Passivating Layer Formation. Environ Sci Technol 40, 4802-4802.
Bobicki, E.R., Liu, Q., Xu, Z., 2015. Mineral carbon storage in pre-treated ultramafic ores. Minerals Engineering 70, 43-54.
Brown, T.C., Mahat, V., Ramirez, J.A., 2019. Adaptation to Future Water Shortages in the United States Caused by Population Growth and Climate Change. Earth's Future 7, 219-234.
Chai, G., Naldrett, A.J., 1992. The Jinchuan Ultramafic Intrusion: Cumulate of a High-Mg Basaltic Magma. Journal of Petrology 33, 277-303.
Clarke, C., Thomas, B., McDonald, J., Blaho, S., Pengel, E., Obermeyer, J., Castendyk, D., Karajeh, I., 2023. Technical Report on the Eagle Mine, Michigan, USA. WSP Golder, Toronto, ON.
Delevingne, L., Glazener, Will, Gregoir, Liesbet, Henderson, Kimberly 2020. Climate risk and decarbonization: What every mining CEO needs to know. McKinsey & Company.
Depp, C.T., Miller, Q.R.S., Crum, J.V., Horner, J.A., Schaef, H.T., 2022. Pore-Scale Microenvironments Control Anthropogenic Carbon Mineralization Outcomes in Basalt. ACS Earth Space Chem. 6, 2836-2847.
Dickinson, D., Berner, P.O., 2010. Ambatovy project: Mining in a challengin biodiversity setting in Madagascar. Malagasy Nature 3, 2-13.

Ding, X., Li, C., Ripley, E.M., Rossell, D., Kamo, S., 2010. The Eagle and East Eagle sulfide ore-bearing mafic-ultramafic intrusions in the Midcontinent Rift System, upper Michigan: Geochronology and petrologic evolution. Geochemistry, Geophysics, Geosystems 11, 1-22.
Donaldson, C.H., 1985. The rates of dissolution of olivine, plagioclase, and quartz in a basalt melt. Mineralogical Magazine 49, 683-693.
Energy, U.S.D.o., 2023. What are critical materials and critical minerals?
Friedrich, B., Marković, B., Sokić, M., Stopić, S., Stanković, S., 2020. Review of the past, present, and future of the hydrometallurgical production of nickel and cobalt from lateritic ores. Metallurgical and Materials Engineering 26, 199-208.
Gao, Y., Jin, X., Teng, L., Rohani, S., He, M., Li, J., Ren, S., Liu, Q., Huang, J., Duan, H., Xin, Y., Liu, W., 2023. CO2 mineral sequestration and nickel recovery from laterite ore by using waste copperas. Fuel 331, 125750.
Gazzetti, E.W., Bandstra, J.Z., Diedrich, T.R., 2023. Valorisation of mine waste as carbon mineralisation feedstock, in: B. Abbasi, J.P.A.F., Tibbett, M. (Eds.), Mine Closure 2023: Proceedings of the 16th International Conference on Mine Closure. Australian Centre for Geomechanics, Reno.
Glotov, A.I., Polyakov, G.V., Hoa, T.T., Balykin, P.A., Akimstev, V.A., Krivenko, A.P., Tolstykh, N.D., Phuong, N.T., Thanh, H.H., Hung, T.Q., Petrova, T.E., 2001. The Ban Phuc Ni-Cu-PGE Deposit Related to the Phanerozoic Komatite-Basalt Association in the Song Da Rift, Northwestern Vietnam. The Canadian Mineralogist 39, 573-589.
Gulley, A.L., 2022. One hundred years of cobalt production in the Democratic Republic of the Congo. Resources Policy 79.
Guyot, F., Daval, D., Dupraz, S., Martinez, I., Menez, B., Sissmann, O., 2011. CO2 geological storage: The environmental mineralogy perspective. C.R. Geosci. 343, 246-259.
Hamilton, J.L., Wilson, S., Morgan, B., Harrison, A.L., Turvey, C.C., Paterson, D.J., Dipple, G.M., Southam, G., 2020a. Accelerating Mineral Carbonation in Ultramafic Mine Tailings via Direct CO2 Reaction and Heap Leaching with Potential for Base Metal Enrichment and Recovery. Economic Geology 115, 303-323.
Hamilton, J.L., Wilson, S., Morgan, B., Turvey, C.C., Paterson, D.J., Jowitt, S.M., McCutcheon, J., Southam, G., 2018a. Fate of transition metals during passive carbonation of ultramafic mine tailings via air capture with potential for metal resource recovery. International Journal of Greenhouse Gas Control 71, 155-167.
Hamilton, J.L., Wilson, S.A., Morgan, B., Harrison, A.L., Turvey, C.C., Paterson, D.J., Dipple, G.M., Southam, G., 2020b. Accelerating mineral carbonation in ultramafic mine tailings via direct CO_2 reaction and heap leaching with potential for base metal enrichment and recovery. Economic Geology 115, 303-323.
Hamilton, J.L., Wilson, S.A., Morgan, B., Turvey, C.C., Paterson, D.J., Jowitt, S.M., McCutcheon, J., Southam, G., 2018b. Fate of transition metals during passive carbonation of ultramafic mine tailings via air capture with potential for metal resource recovery. International Journal of Greenhouse Gas Control 71, 155-167.
Hartman, J.C., Schafrick, I.C., 2004. The relevant internal rate of return. The Engineering Economist 49, 139-158.
Herzberg, C., Vidito, C., Starkey, N.A., 2016. Nickel–cobalt contents of olivine record origins of mantle peridotite and related rocks. American Mineralogist 101, 1952-1966.
Honda-McNeil, M.J., 2022a. A Geometallurgical Approach to Assessing Critical Metal Mobility and Recoverability from Ultramafic Mine Tailings.

Honda-McNeil, M.J., 2022b. A Geometallurgical Approach to Assessing Critical Metal Mobility and Recoverability from Ultramafic Mine Tailings. University of Alberta.
Hund, K., La Porta, D., Fabregas, T.P., Laing, T., Drexhage, J., 2020. Minerals for Climate Action: The Mineral Intensity of the Clean Energy Transition. The World Bank, Washington, DC.
IEA, 2021. The Role of Critical Minerals in Clean Energy Transitions. IEA, Paris.
Jacobs, J.E., Stanfield, C.H., Miller, Q.R.S., Villante, M.A., Marcial, J., Nienhuis, E.T., Silverstein, J.A., Polites, E.G., Bartels, M.F., Gooch, B.T., Liu, J., Thakurta, J., Lahiri, N., Schaef, H.T., 2025. Technoeconomic Potential for Carbon Mineralization with Enhanced Recovery of Critical Minerals in the Pacific Northwest. ACS Sustainable Resource Management.
Jayne, R.S., Wu, H., Pollyea, R.M., 2019. Geologic CO2 sequestration and permeability uncertainty in a highly heterogeneous reservoir. International Journal of Greenhouse Gas Control 83, 128-139.
Katre, S., Ochonma, P., Asgar, H., Nair, A.M., Ravi, K., Gadikota, G., 2024. Mechanistic insights into the co-recovery of nickel and iron via integrated carbon mineralization of serpentinized peridotite by harnessing organic ligands. Physical Chemistry Chemical Physics 26, 9264-9283.
Kelemen, P., Matter, J., 2008. In situ carbonation of peridotite for CO2 storage. Proc Natl Acad Sci U S A 105, 17295-17300.
Kelemen, P.B., Hirth, G., 2012. Reaction-driven cracking during retrograde metamorphism: Olivine hydration and carbonation. Earth and Planetary Science Letters 345-348, 81-89.
Krevor, S.C., Graves, C.R., Van Gosen, B.S., MCCafferty, A.E., 2009. Mapping the mineral resource base for mineral carbon-dioxide sequestration in the conterminous United States, U.S. Geological Survey Digital Data Series 414.
Küng, L., Aeschlimann, S., Charalambous, C., McIlwaine, F., Young, J., Shannon, N., Strassel, K., Maesano, C.N., Kahsar, R., Pike, D., van der Spek, M., Garcia, S., 2023. A roadmap for achieving scalable, safe, and low-cost direct air carbon capture and storage. Energy & Environmental Science, 1-25.
Lahiri, N., Miller, Q.R.S., Cao, R., Depp, C.T., Schaef, H.T., 2023. Facile Metal Release from Pore-Lining Phases Enables Unique Carbonate Zonation in a Basalt Carbon Mineralization Demonstration. Environ Sci Technol 57, 11843-11851.
Lammers, L.N., Duan, Y., Anaya, L., Koishi, A., Lopez, R., Delima, R., Jassby, D., Sedlak, D.L., 2023. Electrolytic Sulfuric Acid Production with Carbon Mineralization for Permanent Carbon Dioxide Removal. ACS Sustain Chem Eng 11, 4800-4812.
Langenbruch, C., Zoback, M.D., 2016. How will induced seismicity in Oklahoma respond to decreased saltwater injection rates? Science Advances 2, 1-9.
Le Vaillant, M., Barnes, S.J., Mole, D.R., Fiorentini, M.L., Laflamme, C., Denyszyn, S.W., Austin, J., Patterson, B., Godel, B., Hicks, J., Mao, Y.-J., Neaud, A., 2020. Multidisciplinary study of a complex magmatic system: The Savannah Ni-Cu-Co Camp, Western Australia. Ore Geology Reviews 117.
Li, C., Ripley, E.M., Maier, W.D., Gomwe, T.E.S., 2002. Olivine and sulfur isotopic compositions of the Uitkomst Ni-Cu-sulfide ore-bearing complex, South Africa: evidence for sulfur contamination and multiple magma emplacements. Chemical Geology 188, 149-159.
Li, C., Ripley, E.M., Naldrett, A.J., 2003. Compositional Variations of Olivine and Sulfur Isotopes in the Noril'sk and Talnakh Intrusions, Siberia: Implications for Ore-Forming Processes in Dynamic Magma Conduits. Economic Geology 98, 69-86.
Li, J., Hitch, M., Power, I., Pan, Y., 2018. Integrated Mineral Carbonation of Ultramafic Mine Deposits—A Review. Minerals 8.

Li, X., Nienhuis, E.T., Nagurney, A.B., Miller, Q.R., Zhang, X., Schaef, H.T., 2023. Resolving Nanoscale Processes during Carbon Mineralization Using Identical Location Transmission Electron Microscopy. Environmental Science & Technology Letters.
Liu, J., Martin, P.F., McGrail, B.P., 2021. Rare-earth element extraction from geothermal brine using magnetic core-shell nanoparticles-techno-economic analysis. Geothermics 89, 1-9.
Luolavirta, K., Hanski, E., Maier, W., Santaguida, F., 2018. Whole-rock and mineral compositional constraints on the magmatic evolution of the Ni-Cu-(PGE) sulfide ore-bearing Kevitsa intrusion, northern Finland. Lithos 296-299, 37-53.
Maier, W.D., Barnes, S.-J., Sarkar, A., Ripley, E., Li, C., Livesey, T., 2010. The Kabanga Ni sulfide deposit, Tanzania: I. Geology, petrography, silicate rock geochemistry, and sulfur and oxygen isotopes. Mineralium Deposita 45, 419-441.
Mansur, E.T., Ferreira Filho, C.F., 2016. Magmatic structure and geochemistry of the Luanga Mafic–Ultramafic Complex: Further constraints for the PGE-mineralized magmatism in Carajás, Brazil. Lithos 266-267, 28-43.
Matter, J., Stute, M., Snaebjornsdottir, S.O., Oelkers, E.H., Gislason, S.R., Aradottir, E.S., Sigfusson, B., Gunnarsson, I., Sigurdardottir, H., Gunnlaugsson, E., Axelsson, G., Alfredsson, H.A., Wolff-Boenisch, D., Mesfin, K.G., Fernandex de la Reguera Taya, D., Hall, J., Dideriksen, K., Broecker, W., 2016. Rapid carbon mineralization for permanent disposal of anthropogenic carbon dioxide emissions. Science 352, 1312-1314.
Matter, J.M., Kelemen, P.B., 2009. Permanent storage of carbon dioxide in geological reservoirs by mineral carbonation. Nature Geoscience 2, 837-841.
McGrail, B.P., Schaef, H.T., Spane, F.A., Horner, J.A., Owen, A.T., Cliff, J.B., Qafoku, O., Thompson, C.J., Sullivan, E.C., 2017. Wallula Basalt Pilot Demonstration Project: Post-injection Results and Conclusions. Energy Procedia 114, 5783-5790.
McRea, M.E., 2023. Nickel, USGS Mineral Commodity Summary.
Miller, J.D., Green, J.C., Severson, M.J., Chandler, V.W., Hauck, S.A., Peterson, D.M., Wahl, T.E., 2002. Geology and Mineral Potential of the Duluth Complex and Related Rocks of Northeastern Minnesota, Report of Investigations 58 ISSN 0076-9177. University of Minnesota-Saint Paul.
Morfin, A.M., Stanfield, C.H., Murchland, M.A., Bartels, M.F., Nagurney, A.B., Miller, Q.R.S., Schaef, H.T., 2024. Structure–Composition Relationships for Mg–Ni and Mg–Fe Olivine. ACS Earth Space Chem. 8, 1713-1724.
Morse, I., 2019. Mining turned Indonesian seas red. The drive for greener cars could herald a new toxic tide., The Washington Post, Washington, DC.
Mudd, G.M., 2010. Global trends and environmental issues in nickel mining: Sulfides versus laterites. Ore Geology Reviews 38, 9-26.
Mudd, G.M., Jowitt, S.M., 2022. The New Century for Nickel Resources, Reserves, and Mining: Reassessing the Sustainability of the Devil's Metal. Economic Geology 117, 1961-1983.
Mungall, J.E., Harvey, J.D., Balch, S.J., Azar, B., Atkinson, J., Hamilton, M.A., 2010. Eagle's Nest: A Magmatic Ni-Sulfide Deposit in the James Bay Lowlands, Ontario, Canada Special Publications of the Society of Economic Geologists: The Challenge of Finding New Mineral Resources: Global Metallogeny, Innovative Exploration, and New Discoveries. Society of Economic Geologists, pp. 539-557.
Murchland, M.A., Nagurney, A.B., Lahiri, N., Engelhard, M.H., Schaef, H.T., Miller, Q.R.S., 2023. V23B-0164: Concurrent Carbon Mineralization and Critical Metal Mobilization in Eagle

Intrusion Peridotites, AGU Annual Fall Meeting 2023. American Geophysical Union, San Francisco, California.
Peters, M., Timmerhaus, K., West, R., 2002. Plant Design Economics for Chemical Engineers, 5th Edition ed. McGraw Hill, New York.
Pogge von Strandmann, P.A.E., Burton, K.W., Snaebjornsdottir, S.O., Sigfusson, B., Aradottir, E.S., Gunnarsson, I., Alfredsson, H.A., Mesfin, K.G., Oelkers, E.H., Gislason, S.R., 2019. Rapid CO(2) mineralisation into calcite at the CarbFix storage site quantified using calcium isotopes. Nat Commun 10, 1983.
Polites, E.G., Schaef, H.T., Horner, J.A., Owen, A.T., Holliman, J.E., Jr., McGrail, B.P., Miller, Q.R.S., 2022a. Exotic Carbonate Mineralization Recovered from a Deep Basalt Carbon Storage Demonstration. Environ Sci Technol 56, 14713-14722.
Polites, E.G., Schaef, H.T., Horner, J.A., Owen, A.T., Holliman Jr, J.E., McGrail, B.P., Miller, Q.R.S., 2022b. Exotic Carbonate Mineralization Recovered from a Deep Basalt Carbon Storage Demonstration. Environ. Sci. Technol. 56, 14713-14722.
Power, I.M., Paulo, C., Rausis, K., 2024a. The Mining Industry's Role in Enhanced Weathering and Mineralization for CO(2) Removal. Environ Sci Technol 58, 43-53.
Power, I.M., Paulo, C., Rausis, K., 2024b. The Mining Industry's Role in Enhanced Weathering and Mineralization for CO_2 Removal. Environ. Sci. Technol. 58, 43-53.
Quaresma, V.S., Aguiar, V.M.C., Bastos, A.C., Oliveira, K.S., Vieira, F.V., Sá, F., Baptista Neto, J.A., 2021. The impact of trace metals in marine sediments after a tailing dam failure: the Fundão dam case (Brazil). Environmental Earth Sciences 80.
Santos, R.M., Van Audenaerde, A., Chiang, Y.W., Iacobescu, R.I., Knops, P., Van Gerven, T., 2015. Nickel Extraction from Olivine: Effect of Carbonation Pre-Treatment. Metals 5, 1620-1644.
Schaef, H.T., McGrail, B.P., Owen, A.T., Arey, B.W., 2013. Mineralization of basalts in the CO2–H2O–H2S system. International Journal of Greenhouse Gas Control 16, 187-196.
Simate, G.S., Ndlovu, S., 2014. Acid mine drainage: Challenges and opportunities. Journal of Environmental Chemical Engineering 2, 1785-1803.
Snaebjornsdottir, S.O., Sigfusson, B., Marieni, C., Goldberg, D., Gislason, S.R., Oelkers, E.H., 2020. Carbon dioxide storage through mineral carbonation. Nature Reviews Earth & Environment 1, 90-102.
Stanfield, C.H., Miller, Q.R.S., Battu, A.K., Lahiri, N., Nagurney, A.B., Cao, R., Nienhuis, E.T., DePaolo, D.J., Latta, D.E., Schaef, H.T., 2024. Carbon Mineralization and Critical Mineral Resource Evaluation Pathways for Mafic–Ultramafic Assets. ACS Earth Space Chem. 8, 1204-1213.
Taranovic, V., Ripley, E.M., Li, C., Rossell, D., 2015. Petrogenesis of the Ni–Cu–PGE sulfide-bearing Tamarack Intrusive Complex, Midcontinent Rift System, Minnesota. Lithos 212-215, 16-31.
Templeton, D.C., Schoenball, M., Layland-Bachmann, C.E., Foxall, W., Guglielmi, Y., Kroll, K.A., Burghardt, J.A., White, J.A., 2021. A project lifetime approach to the management of induced seismicty risk at geologic carbon storage sites. Seismological Research Letters.
Thakurta, J., Ripley, E.M., Li, C., 2008. Geochemical constraints on the origin of sulfide mineralization in the Duke Island Complex, southeastern Alaska. Geochemistry, Geophysics, Geosystems 9, 1-34.
Trost, J.N., Dunn, J.B., 2023. Assessing the feasibility of the Inflation Reduction Act's EV critical mineral targets. Nature Sustainability, 1-8.

Verma, R.L., Borongan, G., 2022. Emissions of Greenhouse Gases from Municipal Solid Waste Management System in Ho Chi Minh City of Viet Nam. Urban Science 6.

Wang, B., Zeyen, N., Wilson, S., Honda-McNeil, M.J., Hamilton, J.L., Von Gunten, K., Alessi, D.S., Jones, T.R., Paterson, D.J., Southam, G., 2024. Migration of transition metals and potential for carbon mineralization during acid leaching of processed kimberlite from Venetia diamond mine, South Africa. Applied Geochemistry 166, 105986.

Wang, F., Dreisinger, D., 2022a. Carbon mineralization with concurrent critical metal recovery from olivine. 119, e2203937119.

Wang, F., Dreisinger, D., 2022b. Carbon mineralization with concurrent critical metal recovery from olivine. Proceedings of the National Academy of Sciences of the United States of America 119, 1-7.

Wang, F., Dreisinger, D., 2022c. Carbon mineralization with concurrent critical metal recovery from olivine. Proc. Natl. Acad. Sci. U.S.A. 119, e2203937119.

Wang, F., Dreisinger, D., 2023a. Enhanced CO2 mineralization and selective critical metal extraction from olivine and laterites. Separation and Purification Technology 321, 124268.

Wang, F., Dreisinger, D., 2023b. An integrated process of CO2 mineralization and selective nickel and cobalt recovery from olivine and laterites. Chemical Engineering Journal 451, 139002.

Wang, F., Dreisinger, D., Barr, G., 2023a. Accelerated CO2 Mineralization and Simultaneous Critical Metal Recovery from Ultramafic Tailings, Proceedings of the 62nd Conference of Metallurgists, COM 2023. Springer Nature Switzerland, Cham, pp. 45-53.

Wang, F., Dreisinger, D., Xiao, Y., 2023b. Accelerated CO2 mineralization and utilization for selective battery metals recovery from olivine and laterites. Journal of Cleaner Production 393, 136345.

White, S.K., Spane, F.A., Schaef, H.T., Miller, Q.R.S., White, M.D., Horner, J.A., McGrail, B.P., 2020. Quantification of CO2 Mineralization at the Wallula Basalt Pilot Project. Environ Sci Technol 54, 14609-14616.

Wicks, D., King, J., 2021. Sequestering Carbon with Hybrid Employment of Mineral Assets, CO2 Mineralization for in situ Storage and ex situ Enhanced Metals Recovery Workshop.

Wilson, S., Hamilton, J.L., 2022. Fizzy ore processing sequesters CO_2 while supplying critical metals. Proceedings of the National Academy of Sciences 119, e2212424119.

Wilson, S., Turvey, C., Hamilton, J.L., Power, I.M., Hussain, A., 2023. Critical Metals and the Need for Low CO 2 Mining Poster, AGU23. AGU.

Wilson, S.A., Harrison, A.L., Dipple, G.M., Power, I.M., Barker, S.L.L., Ulrich Mayer, K., Fallon, S.J., Raudsepp, M., Southam, G., 2014. Offsetting of CO2 emissions by air capture in mine tailings at the Mount Keith Nickel Mine, Western Australia: Rates, controls and prospects for carbon neutral mining. International Journal of Greenhouse Gas Control 25, 121-140.

Zang, A., Zimmermann, G., Hofmann, H., Stephansson, O., Min, K.-B., Kim, K.Y., 2018. How to Reduce Fluid-Injection-Induced Seismicity. Rock Mechanics and Rock Engineering 52, 475-493.

Zhang, N., Yang, R., Huang, H.D., Meng, J., Zhang, W., Park, A.-H.A., Moment, A., 2025. Integrated Recovery of Iron and Nickel from Olivine Ores Using Solvent Extraction: Synergistic Production of Amorphous Silica and Carbonates through pH Adjustment and Carbon Mineralization. ACS ES&T Eng. 5, 103-114.

Supporting Information

Carbon-negative nickel mining to meet global mineral resource demands

Quin R.S. Miller [1], Alexandra B. Nagurney [1], Madalyn S. Blondes [2], Joyashish Thakurta [3], Jian Liu [1], Greeshma Gadikota [4], Nabajit Lahiri [1], H. Todd Schaef [1]

[1] Energy and Environment Directorate, Pacific Northwest National Laboratory, Richland, WA, 99352, United States

[2] U.S. Geological Survey, Geology, Energy & Minerals Science Center, Reston, VA 20192, United States

[3] Natural Resources Research Institute, University of Minnesota Duluth, Duluth, MN 55811, United States

[4] School of Civil and Environmental Engineering, Cornell University, Ithaca, NY 14853, United States

S1 Fraction of Reactive Rock Calculation

Fraction Reactive Rock:

Considering that it is unlikely that 100% of any intrusion will react with injected CO_2, we determined a fraction of reactive rock that will react with the injected CO_2. This estimation of reactive rock is a value that combines mineralogy and porosity to determine the amount of rock available to react with the injected CO_2. This reactive rock exists at grain boundaries and fractures in the rock. It was determined based on the following parameters.

Mineralogy: Magmatic ultramafic rocks are 40-100% olivine. Olivine in magmatic ultramafic rocks can contain significant (500-5000 ppm) Ni (Barnes et al., 2023). Of the other major silicate phases in ultramafic rocks, orthopyroxene contains Ni, but at lower concentrations than olivine (Podvin, 1988) and plagioclase contains effectively no Ni. Therefore, olivine is considered as the only reactive mineral, as the objective of these calculations is to determine the amount of Ni that could be released from olivine during its carbonation. While sulfide minerals may contain appreciable amounts of Ni (up to ~34 wt% in pentlandite) (Misra and Fleet, 1973), their composition, texture, and abundance are highly variable in ultramafic rocks (Hauck et al., 1997), and it is not currently known how injected CO_2 will react with sulfide minerals. Therefore, for simplification, sulfide minerals are not considered in this calculation.

Porosity: Porosity measurements of ultramafic rocks range from 0.8% in a serpentinized peridotite (Hyndman and Drury, 1976), 1.0% in gabbro (Hyndman and Drury, 1976), 1.4% in troctolite (Tutolo et al., 2016), 1-4% in dunite (Braun and Kelemen, 2002), and 6-8% in peridotite, primarily as inter- and intragranular microfractures (Hövelmann et al., 2012).

Carbonated Outcrop Veins: In the Oman Ophiolite, a natural example of carbon mineralization in ultramafic peridotite, carbonate veins form in peridotites. Far from active springs, the average carbonate vein volume in peridotite is 1%, and closer to springs the carbonate vein volume is 5% (Kelemen and Matter, 2008).

The above calculation does not take permeability or porosity enhancement by hydraulic fracturing into account. Therefore, we assume a value of 0.05 for the fraction of reactive rock, based on the natural samples described above.

S2 Determination of Rate Limiting Step

Methods

Olivine Dissolution Rate:

The dissolution of olivine and other minerals in contact with CO_2 has been well studied, but is dependent on many factors including: temperature, pressure, grain size, etc. (Oelkers et al., 2018; Rimstidt et al., 2012). For this study, we utilize the surface area normalized forsterite dissolution rate (log r_{geo}) for pH , 5.6 and 0ºC < T (temperature) < 150ºC (Rimstidt et al., 2012):

$$\log r_{geo} = 6.05(0.22) - 0.46(0.02)pH - 3683.0(63.6)1/T \qquad \text{(S1)}$$

For a pH = 4 and T = 90°C, the olivine dissolution rate is 3.16 x 10^{-9} mol / m^2 sec.

CO_2 Mineralization (Carbonation) Rate:

Like the dissolution rate, there have been numerous studies to determine the carbonation rate of olivine, and carbonation rates are also dependent on factors such as temperature, pressure, grain size, etc. (Miller et al., 2019; Sendula et al., 2021). The Wallula Basalt Pilot Demonstration remains the only field test site of $scCO_2$ into basalt (McGrail et al., 2017). Hydrogeologic analysis revealed that 60% of the injected CO_2 was mineralized 2 years post injection (White et al., 2020). Therefore, it can be interpreted that $scCO_2$ mineralization in basalt and ultramafic rocks should be relatively rapid and it can be assumed that all injected CO_2 will mineralize.

Comparison of CO_2 Injection Rate and Olivine Dissolution Rate:

To determine the rate limiting step for our technology, the CO_2 injection rate was compared to the amount of olivine dissolved per year ($r_{diss,yr}$, mol/yr), which was calculated based on the mass reactive rock (m_{RR}, g), specific surface area (A_{geo}, m^2/g), and 3.15 x 10^7 seconds / yr (Equation S2). The olivine dissolution rate was then utilized to determine the amount of Ni produced per year ($m_{Ni,yr}$, g/yr) (Equation S3) and the amount of CO_2 stored per year ($m_{CO_2,yr}$, g/yr) (Equation S4). Here M_{Fo} = molar mass of forsterite (g), X_{Ni} = proportion Ni in the rock, M_{CO_2}= molar mass of CO_2, and 2 is based on the amount of carbonate minerals formed via Equation 1. We use a value of 3000 ppm Ni in olivine and 0.00974 m^2/g for the specific surface area (Bailey, 1976).

Amount of Olivine Dissolved Per Year:

$$r_{diss,yr} = m_{RR} * A_{geo} * r_{geo} * 3.15x10^7 \qquad \text{(S2)}$$

Amount of Ni Produced Per Year:

$$m_{Ni,yr} = r_{diss,yr} * M_{Fo} * X_{Ni} \qquad \text{(S3)}$$

Amount of CO_2 Stored Per Year:

$$m_{CO_2,yr} = r_{diss,yr} * 2 * M_{CO_2} \qquad \text{(S4)}$$

Results

Amount of Ni Produced Per Year: Based on Equation S2, the amount of Ni that could be produced per year, assuming 100% of the rock reacts, is 1,400,000 MT Ni / yr. Considering the total amount of Ni in the rock (1,000,000 MT Ni), it would take ~9 months to release all of the Ni in the rock, based on the dissolution rate and surface area from (Rimstidt et al., 2012).

Amount of CO_2 Stored Per Year: From Equation 11, the amount of CO_2 stored per year, assuming 100% of the rock reacts is 2900 MMT CO_2 / year.

Comparison of CO_2 Stored to CO_2 Injection Rate: The rate of CO_2 storage (2900 MMT / yr) is >1000x the CO_2 injection rate (1.9 MMT / yr) into the 1 km^3 intrusion. While the CO_2 injection rate could likely be increased through increasing the numbers of wells, pump rate, etc., it is unlikely that the CO_2 injection rate could approach the rate of CO_2 mineralization. Therefore, the CO_2 injection rate is the rate limiting step in this technology.

S3 Descriptions of Ultramafic Intrusions Utilized in the Global Assessment of Ultramafic Intrusions for CO_2-EMR Technology

Fourteen mafic-ultramafic intrusions were chosen to explore the potential of the CO_2-EMR technology on real world target assets. These intrusions are described briefly below, but for full data and interpretation of each intrusion, the reader is directed to the studies on that intrusion. This suite of intrusions is diverse in terms of the age of formation, size of intrusion, and resource estimate of sulfide ore. We examine 13 conduit intrusions and one Alaskan style intrusion (Duke Island Intrusion). Alaskan style intrusions are unique from other ultramafic intrusions in that they form small volume intrusions at convergent plate settings, are commonly unlayered mineralogically, and are dominated, when present, by PGE mineralization (Himmelberg and Loney, 1995). This suite of 14 intrusions may not be commonly grouped together in terms of petrologic processes of formation or resource estimate of high-grade sulfide ore. However, each intrusion listed below fits the requirements for the CO_2-EMR technology in that it is an olivine-bearing mafic-ultramafic intrusion and are therefore grouped together in this analysis. Therefore, this work highlights that a diverse suite of magmatic ultramafic intrusions may be the target of the proposed CO_2-EMR technology.

Each of these intrusions contains multiple mafic-ultramafic lithologies, in addition to high-grade sulfide ore (mineralized) bodies. Mafic-ultramafic lithologies in these intrusions include: dunite, peridotite, harzburgite, lherzolite, serpentinized dunite, olivine melatroctolite, picritic gabbro, and olivine pyroxenite. For 12 of the intrusions, a single, dominant, lithology was chosen as a test for the CO_2-EMR technology. For the Tamarack Intrusion, two lithologies were chosen, as described below.

The Duke Island Complex, Alaska, United States is an example of an Alaskan-type mafic-ultramafic complex, which contains a funnel-shaped concentrically zoned intrusive geometry (Himmelberg and Loney, 1995). Lithologies range from Mg-rich at the center of the funnel with an abundance of Mg-rich olivine-bearing rocks such as dunite, to progressively lower Mg-contents and lower olivine contents at the marginal rocks. The sulfide concentrations are highly variable. In the Duke Island Complex, Ni concentrations in olivine in the dunite zone range from 800 ppm to 2400 ppm (Thakurta et al., 2008).

In the Midcontinent Rift region of the United States, related conduit-type magmatic intrusions Eagle in Michigan and Tamarack in Minnesota contain high-grade sulfide ore zones that are rich in Ni. In the peridotite and troctolite rocks of the Eagle deposit about 200 million kilograms of Ni is mineralized in the sulfide zones (Ding et al., 2011). The olivine Ni-content in the melatroctolite ranges from 1700 ppm to 2200 ppm (Ding et al., 2010). In the Tamarack deposit, about 17 million tons of sulfide ore have been estimated with an average content of 1.28 wt.% Ni (Thomas et al., 2022). The Ni-content in olivine in the feldspathic peridotite coarse grained olivine (CGO) intrusion and peridotite bowl intrusion ranges from 1700 ppm to 3000 ppm (Taranovic et al., 2015). The Tamarack Intrusion has received particular interest in the last few years, as Tesla has committed to buying 75,000 MT of Ni from the high-grade ore (Metals, 2022). Therefore, two lithologies, the CGO and the Bowl Intrusion, an olivine sand (Taranovic et al., 2015), were investigated in this study.

In the ultramafic rocks of the Eagle's Nest ultramafic sill complex in the Ring of Fire region of northern Ontario, Canada there is an inferred resource of about 9 million tons of sulfide ore with 1.10 wt.% Ni (Zuccarelli et al., 2022). In the surrounding lherzolite unit, the Ni-content in olivine varies between 1000 ppm and 3000 ppm (Mungall et al., 2010).

The Luanga Complex in Carajas Mineral Province of Brazil is composed of a cluster of small, layered intrusions enriched with disseminated PGE-rich sulfide zones. There is an estimated resource of 142 million tons with 0.11 wt.% Ni (Mansur and Ferreira Filho, 2016). The Ni-content in olivine of the harzburgite ranges between 4,770 ppm and 6,000 ppm (Mansur and Ferreira Filho, 2016).

The Kevitsa deposit in northern Finland is hosted in komatiite, olivine pyroxenite and websterite. There is an estimated resource of 237 million tons of sulfide ore with an average of 0.28% Ni in the sulfide zones (Le Vaillant et al., 2017). The range in the Ni-content of olivine is abnormally high with the greatest values reaching 14,000 ppm (Luolavirta et al., 2018; Yang et al., 2013). A special case of re-equilibration of new batches of olivine with pre-existing Ni-rich sulfides from previous magmatic upheavals has been proposed (Le Vaillant et al., 2017). In the olivine pyroxenite unit, the Ni in olivine content ranges from 100-3650 ppm (Luolavirta et al., 2018)

The Jinchuan Ni-Cu deposit in southwestern margin of the Sino-Korean platform in China has a sulfide ore reserve of about 500 million tons with an average grade of 1.2 wt.% Ni (Chai and Naldrett, 1992). The magmatic intrusion is composed of olivine-bearing ultramafic rocks such as dunite, lherzolite, and olivine pyroxenite. In the peridotite, the Ni-content in the olivine ranges between 1515 ppm and 2485 ppm (Li et al., 2003b).

The Ban Phuc Ni-Cu-PGE sulfide deposit in the Song Da rift of northwestern Vietnam is associated with high-Mg komatiites. There is an estimated 44.4 million tons of sulfide ore in the deposit, with an average grade of 0.52 wt.% (Minerals, 2020). The Ni-content in olivine of the volcanic rocks ranges between 200 and 3,600 ppm (Glotov et al., 2001).

Ni-rich sulfide deposits associated with peridotite and troctolite ultramafic mafic-ultramafic intrusions are found in northwestern Australia. In the Savannah Ni-Cu-Co deposit, 8.02 million tons of sulfide ore reserves have been identified with an average of 1.38 wt.% Ni (2023). The Ni-content in the olivine of the peridotites ranges from 2,000 ppm to 3,100 ppm (Le Vaillant et al., 2020).

The Nkomati (Uitkomst) Complex in northern South Africa has been reported to have 2.9 million tons of massive sulfide ore with 2 wt.% Ni and another 98 million tons of inferred ore with 0.6 wt.% Ni (Li et al., 2002). The rock types include harzburgite, gabbro and pyroxenite. The Ni-content in olivine of the main harzburgite ranges from 2456-4691 ppm (Li et al., 2002).

The Kabanga Nickel deposit in northwest Tanzania is hosted in ultramafic-mafic sill-like intrusions that are part of the larger, Kabanga – Musongati – Kapalagulu belt. Kabanga has an inferred resource of 28.5 million tons of sulfide ore with 2.7 wt.% Ni and the Ni-content in olivine of the harzburgite ranges from 900 to 1800 ppm (Maier et al., 2010).

The magmatic sulfide deposits of the Noril'sk flood-basalt volcanic province in Siberia, Russia are the most productive Ni, Cu, and platinum-group element (PGE) sulfide deposits in the world (Arndt, 2011). In the Noril'sk and Talnakh deposits, the Ni-content in the sulfide ore can be as high as 5 wt.%. In the picritic gabbro host rock of the deposits the Ni in olivine content ranges between 1,200 and 2,200 ppm (Li et al., 2003a).

S4 United States Nickel Resource Estimate

To estimate the total volume of ultramafic rocks in the United States, the surface area of the ultramafic rocks was taken from the 2009 USGS mineral resource base map for carbon dioxide sequestration (Krevor et al., 2009). To determine an average depth, the ultramafic rocks were broken into 6 categories based on tectonic setting and lithology. The following depths of each category were determined from the literature: i) Appalachian ophiolites, which were assumed to have a depth similar to the Baltimore Mafic Complex (Bromery, 1968), ii) Duluth Complex, in which an average depth of 15 km was determined from (Swanson-Hysell et al., 2020) iii) Mid-Continent Rift associated rocks, which are smaller volume intrusions associated with the Duluth Complex (Taranovic et al., 2015), iv) Stillwater Complex (Stanton, 1972), v) West Coast ophiolite complexes (Alexander and Harper, 1992; Gerlach et al., 1981; Saleeby, 1982), and vi) other, generic ultramafic bodies (Thompson and Robinson, 1975). The state, data source identifier, area (m^2) from (Krevor et al., 2009), area (km^2), estimated depth (km), volume (km^3), and category are listed in Table S3. The total volume was then calculated by adding up the volumes of each category (area * depth) for a total of 32,900 km^3.

Table S3: The state, data source identifier from (Krevor et al., 2009), area (km^2), estimated depth (km), volume (km^3), and category for the United States nickel resource estimate.

State	Data Source Identifier	Area (km2)	Depth (km)	Volume (km3)	Category
AR	AR001	0.15	0.5	0.08	Generic ultramafic body
CA	CA001	5585.16	3	16755.48	West Coast ophiolite complexes
	CA002	13.56	3	40.69	West Coast ophiolite complexes
	CA003	68.45	3	205.34	West Coast ophiolite complexes
	CA004	18.95	3	56.86	West Coast ophiolite complexes
CT	CT001	0.56	3	1.68	Appalachians
DE	DE001	1.71	3	5.13	Appalachians
GA	GA001	100.42	3	301.25	Appalachians
	GA002	4.86	3	14.58	Appalachians
ID	ID001	0.51	1	0.51	Mid Continent Rift Intrusion
IL	IL001	0.13	1	0.13	Mid Continent Rift Intrusion
KS	KS001	1.45	1	1.45	Mid Continent Rift Intrusion
KY	KY001	1.13	0.5	0.56	Generic ultramafic body
MA	MA001	4.65	3	13.95	Appalachians
MD	MD001	102.04	3	306.11	Appalachians
MN	MN001	467.36	15	7010.46	Duluth Complex
ME	ME001	176.82	3	530.45	Appalachians
MI	MI001	1.47	1	1.47	Mid Continent Rift Intrusion
MT	MT001	3.40	5.5	18.72	Stillwater Complex
	MT002	7.38	5.5	40.60	Stillwater Complex
	MT003	16.13	5.5	88.71	Stillwater Complex
	MT004	8.56	5.5	47.08	Stillwater Complex
NC	NC001	85.78	3	257.34	Appalachians
NJ	NJ001	3.87	3	11.60	Appalachians
NY	NY001	47.09	3	141.28	Appalachians
NV	NV001	6.08	0.5	3.04	Generic ultramafic body
OR	OR001	1781.75	3	5345.25	West Coast ophiolite complexes
PA	PA001	61.97	3	185.91	Appalachians
SC	SC001	6.64	3	19.91	Appalachians
TN	TN001	0.05	3	0.16	Appalachians

TX	TX001	7.09	0.5	3.55	Generic ultramafic body
VT	VT001	29.06	3	87.18	Appalachians
VA	VA001	74.20	3	222.59	Appalachians
WA	WA001	378.51	3	1135.54	West Coast ophiolite complexes
WI	WI001	5.62	1	5.62	Mid Continent Rift Intrusion
	WI002	6.02	1	6.02	Mid Continent Rift Intrusion
	WI003	1.61	1	1.61	Mid Continent Rift Intrusion
	WI004	1.10	1	1.10	Mid Continent Rift Intrusion
	WI005	20.09	1	20.09	Mid Continent Rift Intrusion
WY	WY001	20.90	0.5	10.45	Generic ultramafic body

References

2023. Savannah Nickel-Copper-Cobalt Mine. NS Energy.

Alexander, R.J., Harper, G.D., 1992. The Josephine ophiolite: an ancient analogue for slow- to intermediate-spreading oceanic ridges. Geological Society of London Special Publications 60, 3-28.

Arndt, N.T., 2011. Insights into the Geologic Setting and Origin of Ni-Cu-PGE Sulfide Deposits of the Norilsk-Talnakh Region, Siberia, Reviews in Economic Geology: Magmatic Ni-Cu and PGE Deposits: Geology, Geochemistry, and Genesis. Society of Economic Geologists.

Bailey, A., 1976. Effects of temperature on the reaction of silicates with aqueous solutions in the low temperature range. Proceedings of the International Symposium on Water-Rock Interaction. Geological Survey Prague, 375-380.

Barnes, S.J., Yao, Z.-S., Mao, Y.-J., Jesus, A.P., Yang, S., Taranovic, V., Maier, W.D., 2023. Nickel in olivine as an exploration indicator for magmatic Ni-Cu sulfide deposits: A data review and re-evaluation. Am. Mineral. 108, 1-17.

Braun, M.G., Kelemen, P.B., 2002. Dunite distribution in the Oman Ophiolite: Implications for melt flux through porous dunite conduits. Geochemistry, Geophysics, Geosystems 3, 1-21.

Bromery, R.W., 1968. Geological interpretation of aeromagnetic and gravity surveys of the northeastern end of the Baltimore-Washington anticlinorium, Hartford, Baltimore and part of Carroll County, Maryland. Johns Hopkins University, Baltimore, Maryland, p. 124.

Chai, G., Naldrett, A.J., 1992. The Jinchuan Ultramafic Intrusion: Cumulate of a High-Mg Basaltic Magma. Journal of Petrology 33, 277-303.

Ding, X., Li, C., Ripley, E.M., Rossell, D., Kamo, S., 2010. The Eagle and East Eagle sulfide ore-bearing mafic-ultramafic intrusions in the Midcontinent Rift System, upper Michigan: Geochronology and petrologic evolution. Geochemistry, Geophysics, Geosystems 11, 1-22.

Ding, X., Ripley, E.M., Li, C., 2011. PGE geochemistry of the Eagle Ni–Cu–(PGE) deposit, Upper Michigan: constraints on ore genesis in a dynamic magma conduit. Mineralium Deposita 47, 89-104.

Gerlach, D.C., Ave Lallemant, H.G., Leeman, W.P., 1981. An island arc origin for the Canyon Mountain Ophiolite complex, eastern Oregon, USA. Earth and Planetary Science Letters 53, 255-265.

Glotov, A.I., Polyakov, G.V., Hoa, T.T., Balykin, P.A., Akimstev, V.A., Krivenko, A.P., Tolstykh, N.D., Phuong, N.T., Thanh, H.H., Hung, T.Q., Petrova, T.E., 2001. The Ban Phuc Ni-Cu-PGE Deposit Related to the Phanerozoic Komatite-Basalt Association in the Song Da Rift, Northwestern Vietnam. The Canadian Mineralogist 39, 573-589.

Hauck, S.A., Severson, M.J., Zanko, L.M., Barnes, S.J., Morton, P., Alminas, H.V., Foord, E.E., Dahlberg, E.H., 1997. An overview of the geology and oxide, sulfide, and platinum-group element mineralization along the western and northern contacts of the Duluth Complex, Middle Proterozoic to Cambrian rifting, central North America.

Himmelberg, G.R., Loney, R.A., 1995. Characteristics and Petrogenesis of Alaskan-type Ultramafic-mafic Intrusions, Southeastern Alaska. U.S. Geological Survey professional paper, 1-47.

Hövelmann, J., Austrheim, H., Jamtveit, B., 2012. Microstructure and porosity evolution during experimental carbonation of a natural peridotite. Chemical Geology 334, 254-265.

Hyndman, R.D., Drury, M.J., 1976. The physical properties of oceanic basement rocks from deep drilling on the Mid-Atlantic Ridge. Journal of Geophysical Research 81, 4042-4052.

Kelemen, P., Matter, J., 2008. In situ carbonation of peridotite for CO2 storage. Proc Natl Acad Sci U S A 105, 17295-17300.

Krevor, S.C., Graves, C.R., Van Gosen, B.S., MCCafferty, A.E., 2009. Mapping the mineral resource base for mineral carbon-dioxide sequestration in the conterminous United States, U.S. Geological Survey Digital Data Series 414.

Le Vaillant, M., Barnes, S.J., Mole, D.R., Fiorentini, M.L., Laflamme, C., Denyszyn, S.W., Austin, J., Patterson, B., Godel, B., Hicks, J., Mao, Y.-J., Neaud, A., 2020. Multidisciplinary study of a complex magmatic system: The Savannah Ni-Cu-Co Camp, Western Australia. Ore Geology Reviews 117.

Le Vaillant, M., Hill, J., Barnes, S.J., 2017. Simplifying drill-hole domains for 3D geochemical modelling: An example from the Kevitsa Ni-Cu-(PGE) deposit. Ore Geology Reviews 90, 388-398.

Li, C., Ripley, E.M., Maier, W.D., Gomwe, T.E.S., 2002. Olivine and sulfur isotopic compositions of the Uitkomst Ni-Cu-sulfide ore-bearing complex, South Africa: evidence for sulfur contamination and multiple magma emplacements. Chemical Geology 188, 149-159.

Li, C., Ripley, E.M., Naldrett, A.J., 2003a. Compositional Variations of Olivine and Sulfur Isotopes in the Noril'sk and Talnakh Intrusions, Siberia: Implications for Ore-Forming Processes in Dynamic Magma Conduits. Economic Geology 98, 69-86.

Li, C., Xu, Z., de Waal, S.A., Ripley, E.M., Maier, W.D., 2003b. Compositional variations of olivine from the Jinchuan Ni–Cu sulfide deposit, western China: implications for ore genesis. Mineralium Deposita 39, 159-172.

Luolavirta, K., Hanski, E., Maier, W., Santaguida, F., 2018. Whole-rock and mineral compositional constraints on the magmatic evolution of the Ni-Cu-(PGE) sulfide ore-bearing Kevitsa intrusion, northern Finland. Lithos 296-299, 37-53.

Maier, W.D., Barnes, S.-J., Sarkar, A., Ripley, E., Li, C., Livesey, T., 2010. The Kabanga Ni sulfide deposit, Tanzania: I. Geology, petrography, silicate rock geochemistry, and sulfur and oxygen isotopes. Mineralium Deposita 45, 419-441.

Mansur, E.T., Ferreira Filho, C.F., 2016. Magmatic structure and geochemistry of the Luanga Mafic–Ultramafic Complex: Further constraints for the PGE-mineralized magmatism in Carajás, Brazil. Lithos 266-267, 28-43.

McGrail, B.P., Schaef, H.T., Spane, F.A., Horner, J.A., Owen, A.T., Cliff, J.B., Qafoku, O., Thompson, C.J., Sullivan, E.C., 2017. Wallula Basalt Pilot Demonstration Project: Post-injection Results and Conclusions. Energy Procedia 114, 5783-5790.

Metals, T., 2022. Tesla and Talon Metals Enter into Supply Agreement for Nickel.

Miller, Q.R.S., Schaef, H.T., Kaszuba, J.P., Gadikota, G., McGrail, B.P., Rosso, K.M., 2019. Quantitative Review of Olivine Carbonation Kinetics: Reactivity Trends, Mechanistic Insights, and Research Frontiers. Environ. Sci. & Technol. Lett. 6, 431-442.

Minerals, B., 2020. Blackstone positions Ta Khao Nickel-Cu-PGE Project for Li-ion battery market with positive Scoping Study.

Misra, K.C., Fleet, M.E., 1973. The chemical compositions of synthetic and natural pentlandite assemblages. Economic Geology 68, 518-539.

Mungall, J.E., Harvey, J.D., Balch, S.J., Azar, B., Atkinson, J., Hamilton, M.A., 2010. Eagle's Nest: A Magmatic Ni-Sulfide Deposit in the James Bay Lowlands, Ontario, Canada Special Publications of the Society of Economic Geologists: The Challenge of Finding New Mineral Resources: Global Metallogeny, Innovative Exploration, and New Discoveries. Society of Economic Geologists, pp. 539-557.

Oelkers, E.H., Declercq, J., Saldi, G.D., Gislason, S.R., Schott, J., 2018. Olivine dissolution rates: A critical review. Chemical Geology 500, 1-19.

Podvin, P., 1988. Ni-Mg partitioning between synthetic olivines and orthopyroxenes: Application to geothermometry. American Mineralogist 73, 274-280.
Rimstidt, J.D., Brantley, S.L., Olsen, A.A., 2012. Systematic review of forsterite dissolution rate data. Geochim. Cosmochim. Acta 99, 159-178.
Saleeby, J.B., 1982. Polygenetic ophiolite belt of the California Sierra Nevada: Geochronological and tectonostratigraphic development. Journal of Geophysical Research 87, 1803-1824.
Sendula, E., Lamadrid, H.M., Rimstidt, J.D., Steele-MacInnis, M., Sublett, D.M., Aradi, L.E., Szabó, C., Caddick, M.J., Zajacz, Z., Bodnar, R.J., 2021. Synthetic Fluid Inclusions XXIV. In situ Monitoring of the Carbonation of Olivine Under Conditions Relevant to Carbon Capture and Storage Using Synthetic Fluid Inclusion Micro-Reactors: Determination of Reaction Rates. Frontiers in Climate 3.
Stanton, R.L., 1972. Ores of Mafic and Ultramafic Association, Ore Petrology. McGraw Hill, pp. 305-351.
Swanson-Hysell, N.L., Hoaglund, S.A., Crowley, J.L., Schmitz, M.D., Zhang, Y., Miller, J.D., 2020. Rapid emplacement of massive Duluth Complex intrusions within the North American Midcontinent Rift. Geology 49, 185-189.
Taranovic, V., Ripley, E.M., Li, C., Rossell, D., 2015. Petrogenesis of the Ni–Cu–PGE sulfide-bearing Tamarack Intrusive Complex, Midcontinent Rift System, Minnesota. Lithos 212-215, 16-31.
Thakurta, J., Ripley, E.M., Li, C., 2008. Geochemical constraints on the origin of sulfide mineralization in the Duke Island Complex, southeastern Alaska. Geochemistry, Geophysics, Geosystems 9, 1-34.
Thomas, B., Jackson, R., Peters, O., Pint, C., 2022. November 2022 National Instrument 43-101 Technical Report of the Tamarack Noth Project- Tamarack, Minnesota, in: Golder, W. (Ed.). Talon Metals Corp.
Thompson, G.A., Robinson, R., 1975. Gravity and magnetic investigation of the Twin Sisters Dunite, Northern Washington. Geological Society of America Bulliten 86, 1413-1422.
Tutolo, B.M., Mildner, D.F.R., Gagnon, C.V.L., Saar, M.O., Seyfried, W.E., 2016. Nanoscale constraints on porosity generation and fluid flow during serpentinization. Geology 44, 103-106.
White, S.K., Spane, F.A., Schaef, H.T., Miller, Q.R.S., White, M.D., Horner, J.A., McGrail, B.P., 2020. Quantification of CO_2 Mineralization at the Wallula Basalt Pilot Project. Environ Sci Technol 54, 14609-14616.
Yang, S.-H., Maier, W.D., Hanski, E.J., Lappalainen, M., Santaguida, F., Määttä, S., 2013. Origin of ultra-nickeliferous olivine in the Kevitsa Ni–Cu–PGE-mineralized intrusion, northern Finland. Contributions to Mineralogy and Petrology 166, 81-95.
Zuccarelli, N., Lesher, C.M., Houlé, M.G., Weston, R., Barnes, S.J., 2022. Diversity of Net-Textured Sulfides in Magmatic Sulfide Deposits: Insights from the Eagle’s Nest Ni-Cu-(Platinum Group Element) Deposit, McFaulds Lake Greenstone Belt, Superior Province, Canada. Economic Geology 117, 1731-1759.